arXiv:1402.5604v1 [cs.SY] 23 Feb 2014

Three-Dimensional Integrated Guidance and Control Based on Small-Gain Theorem*

Han Yan†

Science and Technology on Space Intelligent Control Laboratory,

Beijing Institute of Control Engineering, Beijing 100190, China

and

Mingzhe Hou‡

Center for Control Theory and Guidance Technology,

Harbin Institute of Technology, Harbin 150001, China

Abstract: A three-dimensional (3D) integrated guidance and control (IGC) design approach is proposed by using small-gain theorem in this paper. The 3D IGC model is formulated by combining nonlinear pursuer dynamics with the nonlinear dynamics describing pursuit-evasion motion. Small-gain theorem and ISS theory are iteratively utilized to design desired attack angle, sideslip angle and attitude angular rates (virtual controls), and eventually an IGC law is proposed. Theoretical analysis shows that the IGC approach can make the LOS rate converge into a small neighborhood of zero, and the stability of the overall system can be guaranteed as well.

Key words: Three-dimensional integrated guidance and control; Generalized small-gain theorem; Input-to-state stability; Robustness.

*This work was supported by National Natural Science Foundation of China (No.61203125) and Fundamental Research Funds for the Central Universities (No. HIT. NSRIF. 2013039).

†Engineer, e-mail address: yhbice@gmail.com.

‡Lecturer, e-mail address: hithyt@gmail.com.

Nomenclature

α	=	angle of attack
β	=	angle of sideslip
γ	=	roll angle
ϑ	=	pitch angle
ω_i $(i = x, y, z)$	=	body-axis roll, yaw and pitch rates
δ_i $(i = x, y, z)$	=	aileron, rudder and elevator deflections
V	=	velocity of the pursuer
m	=	mass of the pursuer
P	=	thrust force
ρ	=	air density
$q = 0.5qV^2$	=	dynamic pressure
J_i $(i = x, y, z)$	=	roll, yaw and pitch moments of inertia
X, Y, Z	=	drag, lift and side forces
S, L	=	reference area, reference length
r	=	relative range between pursuer and evader
θ_L, φ_L	=	LOS elevation, LOS azimuth
θ_V, φ_V	=	velocity elevation, velocity azimuth
c_{x0}	=	zero-lift drag coefficient
F_i $(i = V, \theta, \varphi)$	=	force components along the axes of the velocity coordinate system
$c_x^{\alpha}, c_x^{\beta}$	=	partial derivatives of drag force coefficient with respect to α and β
$c_x^{\delta_x}, c_x^{\delta_y}, c_x^{\delta_z}$	=	partial derivatives of drag force coefficient with respect to δ_x, δ_y and δ_z
$c_x^{\alpha\beta}$	=	second partial derivatives of drag force coefficient with respect to α and β
$c_y^{\alpha}, c_y^{\beta}, c_y^{\delta_z}$	=	partial derivatives of lift force coefficient with respect to α, β and δ_z
$c_z^{\alpha}, c_z^{\beta}, c_y^{\delta_y}$	=	partial derivatives of side force coefficient with respect to α, β and δ_y
$m_x^{\delta_x}, m_x^{\alpha}, m_x^{\beta}$	=	partial derivatives of rolling moment coefficient with respect to δ_x, α and β
$m_y^{\beta}, m_y^{\delta_y}$	=	partial derivatives of yawing moment coefficient with respect to β and δ_y
$m_z^{\alpha}, m_z^{\delta_z}$	=	partial derivatives of pitching moment coefficient with respect to α and δ_z

1 Introduction

The guidance and control systems of vehicles are usually designed separately, and in order to achieve the desired overall system performance, modifications are generally inevitably required to each subsystem. Hence, the traditional design approach usually leads to excessive design iterations and high costs. What's more, strictly speaking, the stability of the overall system cannot be guaranteed [1]. Integrated guidance and control (IGC) design is regarded as one of emerging trends in vehicle control technology, because it views guidance and control loops as an integrated system and taking couplings between subsystems into account, and besides that, such a design can reduce the cost of the required sensors and increase the system reliability [2]. Due to those reasons, IGC design has received more and more attention recently.

After IGC design was put forward in [2], various control methods have been introduced, and sliding-mode control (SMC) is a typical method, which is used in most of the existing relevant literatures to solve the two-dimensional IGC design problem for the pursuit-evasion game. The second-order SMC was used to design IGC laws in [3] and [4]. In [3], a sliding surface that depends on the line-of-sight (LOS) rate was defined in the guidance loop with the pursuer pitch rate viewed as a virtual control, and the second-order SMC was used to control the pitch rate to track the virtual control robustly in finite time. For pursuers steered by a combination of aerodynamic lift, sustainer thrust, and center-of-gravity divert thrusters, an IGC algorithm, integrated with the smooth second-order sliding mode guidance law in [5], was developed using second-order SMC to achieve an accurate tracking of the attitude command [4]. Similarly, [6] also designed the pitch rate command in outer loop, and the inner loop was constructed to track the outer loop command, where the finite time convergence can be guaranteed in both two loops according to the novel adaptive nonsingular terminal SMC method proposed in the paper. Shima and co-workers used SMC to obtain IGC approaches for pursuers with only one control input [7] and pursuers with both canard and tail controls [8] with the assumption that the evader acceleration can be measured. Note that, in order to remove nonlinear terms, the equations of IGC model in [7] and [8] were all formulated under the assumption that the angle

between LOS and pursuer velocity is almost constant, but it might be not proper in practice since large maneuvers of a evader may lead to significant variation of that angle. The IGC laws in [9] and [10] were proposed without that assumption. To deal with the nonlinear terms, an adaptive control method was introduced into the backstepping scheme to design an IGC law [9]. For dual-control pursuers, small-gain theorem [11] was also used to design IGC law in [10] to enforce the attitude angle (rate) commands that are aimed at producing desired aerodynamic lift to achieve robust tracking of a maneuvering evader. Both IGC laws in [9] and [10] can make the LOS rate converge into a small neighborhood of zero in the presence of evader maneuvers and pursuer model uncertainties.

Actually, an actual pursuit-evasion motion occurs in a three-dimensional (3D) environment. Only when the couplings between lateral and normal motion are ignored, the design and analysis of IGC laws can be simplified into two planar relative motions. However, such an approach is ad hoc in nature, and the 3D IGC law design is a challenging problem.

For IGC problem in three dimensions, some nonlinear optimal control methods, such as state dependent Riccati equation (SDRE) technique [12, 13] and $\theta - D$ technique [14], were utilized. These methods all involve complicated numerical computations since the Hamilton-Jaccobi-Bellman (HJB) equation is needed to be solved on-line and that is time consuming. What is more, these methods cannot ensure the robustness of the closed-loop system. Without complicated numerical computations, adaptive block dynamic surface control, which can avoid "explosion of complexity" problem when comparing with backstepping method, was used to design 3D IGC law [1]. A set of first-order filters were introduced at each step of the traditional block backstepping approach, and the stability analysis of the closed-loop system was also given based on the Lyapunov theory. But similarly to [7] and [8], [1] also assumed that the angle between LOS and pursuer velocity is constant.

All the works mentioned above made great contributions to the development of IGC design, but many existing results were obtained based on some strong assumptions or without considering robustness against uncertainties and disturbances. In addition, most of 3D IGC laws involve

complicated numerical computations and cannot stabilize the overall system.

In this paper, a novel 3D IGC design approach is proposed for skid-to-turn (STT) vehicles by iteratively using small-gain theorem and input-to-state stability (ISS) [15]. The desired attack angle and sideslip angle are designed to make the LOS rate be ISS with respect to evader maneuvers. Then, by iteratively utilizing small-gain theorem, the desired attitude angular rates and the final IGC law are proposed to drive the attack angle and sideslip angle to track their commands. Theoretical analysis show that the IGC approach makes both the LOS rate and the tracking error of attitude angle (rate) be input-to-state practically stable (ISpS) with respect to evader maneuvers and pursuer model uncertainties. It is worth to claim that our approach is formulated considering the couplings between lateral and pitch channels, and the nonlinearity caused by the moving between LOS and pursuer velocity is also taken into consideration. Besides, the stability of the overall system can be guaranteed by small-gain theorem, and comparing with the backstepping scheme, the procedures of our design approach do not involve the derivatives of virtual controls, such that the problem of "explosion of complexity" is avoided.

The remainder of this paper is organized as follows. The 3D integrated guidance and control model is formulated in Section 2. After presenting some basic concepts, the IGC law is designed in Section 3, and also stability of the overall pursuer system is analyzed. Finally, Section 4 summarizes the conclusions.

2 Model Derivation

The nonlinear pursuer dynamics with uncertainties proposed in [1] is described by

$$\dot{x}_1 = f_1(x_1) + g_1(\vartheta, x_1)x_2 + d_1 \tag{1a}$$

$$\dot{x}_2 = f_2(x_1, x_2) + g_2(t)u + d_2 \tag{1b}$$

where

$$x_1 = \begin{bmatrix} \gamma \\ \alpha \\ \beta \end{bmatrix},\ x_2 = \begin{bmatrix} \omega_x \\ \omega_y \\ \omega_z \end{bmatrix},\ u = \begin{bmatrix} \delta_x \\ \delta_y \\ \delta_z \end{bmatrix},$$

$$f_1(x_1) = \begin{bmatrix} 0 \\ -\frac{1}{mV\cos\beta}\left(P\sin\alpha + qSC_y^{\alpha}\alpha\right) \\ \frac{1}{mV}\left(qSC_z^{\beta}\beta - P\cos\alpha\sin\beta\right) \end{bmatrix},\ g_1(\vartheta, x_1) = \begin{bmatrix} 1 & -\tan\vartheta\cos\gamma & \tan\vartheta\sin\gamma \\ -\tan\beta\cos\alpha & \sin\alpha\tan\beta & 1 \\ \sin\alpha & \cos\alpha & 0 \end{bmatrix},$$

$$f_2(x_1, x_2) = \begin{bmatrix} \frac{J_z - J_y}{J_x}\omega_y\omega_z \\ \frac{1}{J_y}qSLm_y^{\beta}\beta + \frac{J_x - J_z}{J_y}\omega_x\omega_z \\ \frac{1}{J_z}qSLm_z^{\alpha}\alpha + \frac{J_y - J_x}{J_z}\omega_x\omega_y \end{bmatrix},\ g_2(t) = \begin{bmatrix} \frac{1}{J_x}qSLm_x^{\delta_x} & 0 & 0 \\ 0 & \frac{1}{J_y}qSLm_y^{\delta_y} & 0 \\ 0 & 0 & \frac{1}{J_z}qSLm_z^{\delta_z} \end{bmatrix}$$

and

$$\dot{\vartheta} = \omega_y\sin\gamma + \omega_z\cos\gamma \tag{3}$$

where d_1 and d_2 are uncertainties.

Consider the spherical LOS coordinates (r, θ_L, φ_L) with origin fixed at the pursuer's gravity center. As shown in Fig. 1, let $(\mathbf{e_r}, \mathbf{e_{\theta_L}}, \mathbf{e_{\varphi_L}})$ be the unit vectors along the coordinate axes, r be the relative range between pursuer and evader, θ_L be the LOS elevation, and φ_L be the LOS azimuth. The components of the relative acceleration is given as [1, 17]

$$\ddot{r} = r(\dot{\varphi}_L)^2\cos^2\theta_L + r(\dot{\theta}_L)^2 + a_{E_r} - a_{P_r} \tag{4a}$$

$$\ddot{\theta}_L = \frac{-2\dot{r}\dot{\theta}_L - r(\dot{\varphi}_L)^2\cos\theta_L\sin\theta_L + a_{E_{\theta_L}} - a_{P_{\theta_L}}}{r} \tag{4b}$$

$$\ddot{\varphi}_L = \frac{-2\dot{r}\dot{\varphi}_L}{r} + 2\dot{\varphi}_L\dot{\theta}_L\tan\theta_L + \frac{a_{E_{\varphi_L}} - a_{P_{\varphi_L}}}{r\cos\theta_L} \tag{4c}$$

where $(a_{P_r}, a_{P_{\theta_L}}, a_{P_{\varphi_L}})$ and $(a_{E_r}, a_{E_{\theta_L}}, a_{E_{\varphi_L}})$ are, respectively, the acceleration vectors of pursuer and evader in the LOS coordinate system.

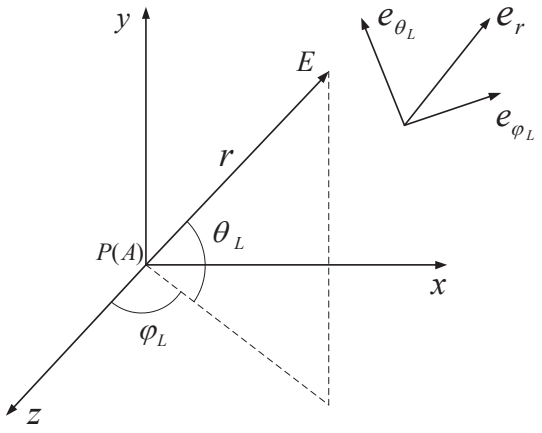

Figure 1: The Pursuit-Evasion Motion

The relationship between ground coordinate system and pursuer velocity coordinate system is shown in Fig. 2, where Ox' axe is along the pursuer velocity vector, θ_V is the velocity elevation, and ψ_V is the velocity azimuth. Let (F_V, F_θ, F_ψ) be the force components along the axes of the velocity coordinate system, and one has [16]

$$ma_V = m\frac{\mathrm{d}V}{\mathrm{d}t} = F_V \tag{5a}$$

$$ma_\theta = mV\frac{\mathrm{d}\theta_V}{\mathrm{d}t} = F_\theta \tag{5b}$$

$$ma_\psi = -mV\cos\theta_V\frac{\mathrm{d}\psi_V}{\mathrm{d}t} = F_\psi \tag{5c}$$

where (a_V, a_θ, a_ψ) is the acceleration vector of the pursuer in velocity coordinate system.

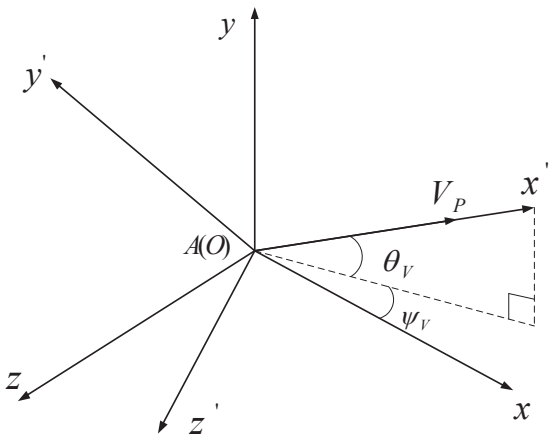

Figure 2: Ground Coordinate System ($Axyz$) and Pursuer Velocity Coordinate System ($Ox'y'z'$)

The vector (x, y, z) in the ground coordinate system can be transformed to the pursuer velocity coordinate system through the following equation [16]

$$\begin{bmatrix} x' \\ y' \\ z' \end{bmatrix} = \mathbf{L}(\psi_V, \theta_V) \begin{bmatrix} x \\ y \\ z \end{bmatrix} \tag{6}$$

where

$$\mathbf{L}(\psi_V, \theta_V) = \begin{bmatrix} \cos\theta_V \cos\psi_V & \sin\theta_V & -\cos\theta_V \sin\psi_V \\ -\sin\theta_V \cos\psi_V & \cos\theta_V & \sin\theta_V \sin\psi_V \\ \sin\psi_V & 0 & \cos\psi_V \end{bmatrix}$$

Therefore, according to Eq. (6) and the definitions of the velocity elevation and azimuth, one can obtain

$$\begin{bmatrix} a_{P_r} \\ a_{P_{\theta_L}} \\ -a_{P_{\varphi_L}} \end{bmatrix} = \mathbf{L}\left(\varphi_L - \frac{\pi}{2}, \theta_L\right) \mathbf{L}^{-1}(\psi_V, \theta_V) \begin{bmatrix} a_V \\ a_\theta \\ a_\psi \end{bmatrix} \tag{7}$$

In practical applications, during the end game, the pursuer speed is usually assumed to be constant, i.e., $a_V = 0$ [7, 8, 10].

The acceleration components of the pursuer along the y- and z-axes of the pursuer velocity coordinate system are given by [16]

$$\begin{bmatrix} a_\theta \\ a_\psi \end{bmatrix} = \frac{1}{m} \begin{bmatrix} P\sin\alpha + Y \\ -P\cos\alpha\sin\beta + Z \end{bmatrix} \tag{8}$$

where lift force Y and side force Z are given by

$$Y = qSC_y^\alpha \alpha + d_y \tag{9a}$$

$$Z = qSC_z^\beta \beta + d_z \tag{9b}$$

with uncertainties d_y and d_z. When α and β are small enough, we have $\sin\alpha \approx \alpha$, $\sin\beta \approx \beta$ and $\cos\alpha \approx 1$. Thus,

$$\begin{bmatrix} a_\theta \\ a_\psi \end{bmatrix} = \frac{1}{m} \begin{bmatrix} P + qSC_y^\alpha & 0 \\ 0 & -P + qSC_z^\beta \end{bmatrix} \begin{bmatrix} \alpha \\ \beta \end{bmatrix} + \underbrace{\frac{1}{m} \begin{bmatrix} d_y \\ d_z \end{bmatrix}}_{d_V} \tag{10}$$

From Eq. (7), we have

$$\begin{bmatrix} a_{P_{\theta_L}} \\ a_{P_{\varphi_L}} \end{bmatrix} = \begin{bmatrix} \sin\theta_L \sin\theta_V \sin(\varphi_L - \psi_V) + \cos\theta_L \cos\theta_V & -\sin\theta_L \cos(\psi_V - \varphi_L) \\ -\sin\theta_V \cos(\varphi_L - \psi_V) & -\sin(\varphi_L - \psi_V) \end{bmatrix} \begin{bmatrix} a_\theta \\ a_\psi \end{bmatrix} \triangleq M(t) \begin{bmatrix} a_\theta \\ a_\psi \end{bmatrix} \tag{11}$$

Define

$$x_{01} = \omega_\theta = \dot{\theta}_L,\ x_{02} = \omega_\phi = \dot{\phi}_L \triangleq \dot{\varphi}_L \cos\theta_L \tag{12}$$

and

$$x_0 = \begin{bmatrix} x_{01} \\ x_{02} \end{bmatrix},\ x_1^\# = \begin{bmatrix} \alpha \\ \beta \end{bmatrix} \tag{13}$$

From (4), (10) and (11), we have

$$\dot{x}_0 = f_0(x_0) + g_0(t)x_1^\# + \frac{d_0(t)}{r} \tag{14}$$

where

$$f_0(x_0) = \begin{bmatrix} -2\frac{V_r}{r}x_{01} - x_{02}^2 \tan\theta_L \\ -2\frac{V_r}{r}x_{02} + x_{01}x_{02}\tan\theta_L \end{bmatrix},\ g_0(t) = -\frac{M(t)}{mr} \begin{bmatrix} P + qSC_y^\alpha & 0 \\ 0 & -P + qSC_z^\beta \end{bmatrix} \tag{15}$$

and $d_0(t) = -M(t)d_V + \begin{bmatrix} a_{E_{\theta_L}} \\ a_{E_{\varphi_L}} \end{bmatrix}$ is assumed to be bounded disturbance.

According to the above analysis, the IGC model can be written as

$$\dot{x}_0 = f_0(x_0) + g_0(t)x_1^{\#} + \frac{d_0}{r} \tag{16a}$$

$$\dot{x}_1 = f_1(x_1) + g_1(\vartheta, x_1)x_2 + d_1 \tag{16b}$$

$$\dot{x}_2 = f_2(x_1, x_2) + g_2(t)u + d_2 \tag{16c}$$

Let $(\mathbf{i}_x, \mathbf{i}_y, \mathbf{i}_z)$ be the unite vectors along the ground coordinate axes, and we can see from Fig. (2) that

$$\boldsymbol{r} = r\cos\theta_L \sin\varphi_L \boldsymbol{i}_x + r\sin\theta_L \boldsymbol{i}_y + r\cos\theta_L \cos\varphi_L \boldsymbol{i}_z \tag{17a}$$

$$\boldsymbol{V}_M = V_M \cos\theta_V \cos\psi_V \boldsymbol{i}_x + V_M \sin\theta_V \boldsymbol{i}_y - V_M \cos\theta_V \sin\psi_V \boldsymbol{i}_z \tag{17b}$$

It is easy to verify that

$$\det(M(t)) = \frac{\boldsymbol{r} \cdot \boldsymbol{V}_M}{r^2 V_M} \tag{18}$$

holds, so when pursuer velocity is orthogonal onto the LOS, we have $\det(M(t)) = 0$, that is, $M(t)$ is non-invertible in this case. But the angle between LOS and pursuer velocity is always acute in the whole process of homing guidance [9], thus we assume that the matrix $M(t)$ is invertible here, and in this case, $g_0(t)$ is invertible. Due to the analysis of [1], if α, β and ϑ are all kept in a reasonable domain around zero, $g_1(\vartheta, x_1)$ is also invertible for arbitrary variable γ, so we assume that $g_1(\vartheta, x_1)$ is invertible in a reasonable flight domain.

3 Integrated Guidance and Control Law Design

In this section, small-gain theorem and ISS theory are iteratively used to design desired attack angle, sideslip angle and attitude angular rates (virtual controls), and eventually an IGC law is proposed. Theoretical analysis shows that the IGC approach can make the LOS rate converge into a small neighborhood of zero, and the stability of the overall system can be guaranteed as well.

For any measurable function $u(t) : \mathbb{R}_+ \to \mathbb{R}^m$, $\|u(t)\|_s$ denotes $\sup_{0\le\tau\le t} \|u(\tau)\|$.

3.1 Concepts and Preliminaries

Consider the following general interconnected system

$$H_1 : \ \dot{x}_1 = f_1(x_1, y_2, u_1), \ y_1 = h_1(x_1, y_2, u_1) \tag{19}$$

$$H_2 : \ \dot{x}_2 = f_2(x_2, y_1, u_2), \ y_2 = h_2(x_2, y_1, u_2) \tag{20}$$

where, for $i = 1, 2$, $x_i \in \mathbb{R}^{n_i}$, $u_i \in \mathbb{R}^{m_i}$, and $y_i \in \mathbb{R}^{p_i}$. The functions f_1, f_2, h_1 and h_2 are smooth and a smooth function h exists such that

$$(y_1, y_2) = h(x_1, x_2, u_1, u_2),$$

is the unique solution of

$$\begin{cases} y_1 = h_1(x_1, h_2(x_2, y_1, u_2), u_1) \\ y_2 = h_2(x_2, h_1(x_1, y_2, u_1), u_2) \end{cases}$$

We have:

Theorem 1 *[11] Suppose (19) and (20) are input-to-state stability (ISS) with (y_2, u_1) (respectively (y_1, u_2)) as input, y_1 (respectively y_2) as output, and there exist class $\mathcal{KL}$ functions β_1, β_2, class $\mathcal{K}$ functions γ_{1y}, γ_{1u}, γ_{2y}, γ_{2u}, and nonnegative constants d_1, d_2 such that*

$$\begin{cases} \|y_1(t)\| \le \beta_1(\|x_1(0)\|, t) + \gamma_{1y}(\|y_2(t)\|_s) + \gamma_{1u}(\|u_1(t)\|_s) + d_1 \\ \|y_2(t)\| \le \beta_2(\|x_2(0)\|, t) + \gamma_{2y}(\|y_1(t)\|_s) + \gamma_{2u}(\|u_2(t)\|_s) + d_2 \end{cases}$$

If two class $\mathcal{K}_\infty$ functions ρ_1 and ρ_2 and a nonnegative real number s_l satisfying

$$\begin{cases} (Id + \rho_2) \circ \gamma_{2y} \circ (Id + \rho_1) \circ \gamma_{1y}(s) \le s \\ (Id + \rho_1) \circ \gamma_{1y} \circ (Id + \rho_2) \circ \gamma_{2y}(s) \le s \end{cases}, \quad \forall s \ge s_l \tag{21}$$

exist, system (19)-(20) with $u = (u_1, u_2)$ as input, $y = (y_1, y_2)$ as output and $x = (x_1, x_2)$ as state will be input-to-output practically stability (IOpS) (input-to-output stability (IOS) if $s_l = d_1 = d_2 = 0$).

3.2 ISS-Based Control Law Design

Consider general nonlinear system

$$\dot{x} = f(x,t) + g(x,t)u + d(t) \tag{22}$$

where $f : [0,\infty) \times R^n \to R^n$, $f : [0,\infty) \times R^n \to R^{n\times n}$ and disturbance $d : [0,\infty) \to R^n$. The following theorem holds.

Theorem 2 *Assume $g(x,t)$ is invertible. The closed-loop system of system (22) and control law*

$$u = g^{-1}\left(-f - kx - \frac{1}{2\delta^2}x\right) \tag{23}$$

is ISS with respect to d for $k > 0$ and $\delta > 0$, that is,

$$\|x(t)\| \le e^{-kt}\|x(0)\| + \frac{\delta}{\sqrt{2k}}\sqrt{1-e^{-2kt}}\|d(t)\|_s \tag{24}$$

Moreover, if disturbance d vanishes, the origin of the closed-loop system will be exponentially stable.

Proof. The derivative of $V = \frac{1}{2}x^Tx$ along the trajectories of system (22) is given by

$$\dot{V} = x^T(f(x,t) + g(x,t)u + d(t)) \tag{25}$$

Applying

$$x^Td \le \frac{1}{2\delta^2}\|x\|^2 + \frac{\delta^2}{2}\|d\|^2 \tag{26}$$

where $\delta > 0$, into (25), we obtain

$$\dot{V} \le x^T\left(f(x,t) + g(x,t)u + \frac{1}{2\delta^2}x\right) + \frac{\delta^2}{2}\|d\|^2 \tag{27}$$

Substituting (23) into Eq. (27) yields

$$\dot{V} \le -k\|x\|^2 + \frac{\delta^2}{2}\|d\|^2 \tag{28}$$

Solving the differential inequality yields

$$V(x(t)) \le e^{-2kt}V(x(0)) + \frac{\delta^2}{4k}(1-e^{-2kt})\|d(t)\|_s^2 \tag{29}$$

Taking the square roots and using the inequality $\sqrt{a^2+b^2} \leq a+b$ for nonnegative numbers a and b, we can see that Eq. (24) holds. Therefore, the closed-loop system of system (22) and control law (23) is ISS with respect to disturbance d.

Moreover, if disturbance d vanishes, that is, $d=0$, Eq. (24) can be rewritten as $\|x(t)\| \leq e^{-kt}\|x(0)\|$. In this case, the origin of the closed-loop system is exponentially stable. □

Theorem 2 shows that, with the control law (23), x can converge to a small neighborhood of zero by adjusting coefficients k and δ for bounded disturbance d.

3.3 IGC Law Design

Consider subsystem (16a). $\frac{d_0}{r}$ is not bounded when $r=0$, however, due to the finite size of pursuers and evaders, a successful interception can be achieved as long as r decreases to a particular intercept value in the whole process of homing guidance. Thus, $\frac{d_0}{r}$ is bounded and we assume that inequality $0<r_m<r<r_M$ holds [5,17]. Since the assumption that g_0 is invertible is reasonable as analyzed, according to Theorem 2, taking the virtual control law[1]

$$x_1^{\#} = g_0^{-1}\left(2\frac{V_r}{r} - \frac{1}{2\delta_0^2} - K_0\right)x_0 \triangleq x_1^{\#*} \tag{30}$$

with $K_0>0$ and $\delta_0>0$, we can obtain

$$\|x_0(t)\| \leq e^{-K_0 t}\|x_0(0)\| + \frac{\delta_0}{\sqrt{2K_0}r_m}\sqrt{1-e^{-2K_0 t}}\|d_0(t)\|_s \tag{31}$$

For STT vehicles, the roll angle should be kept near zero throughout the engagement, thus, let $x_1^* = [0,(x_1^{\#*})^T]^T$, and the change of variables

$$\eta_1^{\#} = x_1^{\#} - x_1^{\#*}, \eta_1 = x_1 - x_1^* \tag{32}$$

brings Eqs. (16a)-(16b) into the form

$$H_1: \begin{cases} \dot{x}_0 = f_0 + g_0 x_1^{\#*} + \dfrac{d_0}{r} + y_1 \\ y_0 = -\dot{x}_1^* \end{cases}$$

[1]The terms $-x_{02}^2\tan\theta_L$ and $x_{01}x_{02}\tan\theta_L$ in f_0 (the cross couplings between the elevation and the azimuth of LOS) need no consideration when designing the virtual control, see [17].

and

$$H_2 : \begin{cases} \dot{\eta}_1 = f_1 + g_1 x_2 + d_1 + y_0 \\ y_1 = g_0 \eta_1^{\#} \end{cases}$$

With $x_1^{\#*}$, system H_1 is ISS with respect to d_0 and y_1, and due to Eq. (31), we have

$$\|x_0(t)\| \leq \underbrace{e^{-K_0 t}\|x_0(0)\|}_{\beta_0^x(\|x_0(0)\|,t)} + \underbrace{\frac{\delta_0}{\sqrt{2K_0}r_m}\sqrt{1-e^{-2K_0 t}}\|d_0(t)\|_s}_{\alpha_0^x(\|d_0(t)\|_s)} + \underbrace{\frac{\delta_0}{\sqrt{2K_0}}\sqrt{1-e^{-2K_0 t}}\|y_1(t)\|_s}_{r_m\alpha_0^x(\|y_1(t)\|_s)} \tag{33}$$

According to Proposition 3.1 of [11], for the output function y_0, the inequality

$$\|y_0(t)\| \leq \gamma_0^u(\|d_0(t)\|_s) + \gamma_0^y(\|y_1(t)\|_s) + \beta_0(\|x_0(0)\|, t) \tag{34}$$

holds for a pair of class $\mathcal{K}$ functions (γ_0^u, γ_0^y) and a class $\mathcal{KL}$ function β_0. We have assumed that g_1 is invertible in a reasonable flight domain, thus, for system H_2, the virtual control law

$$x_2 = g_1^{-1}\left(-f_1 - \frac{1}{2\delta_1^2}\eta_1 - K_1\eta_1\right) \triangleq x_2^* \tag{35}$$

with $K_1 >$ and $\delta_1 > 0$ can be also designed based on Theorem 2 such that

$$\|\eta_1(t)\| \leq e^{-K_1 t}\|\eta_1(0)\| + \frac{\delta_1}{\sqrt{2K_1}}\sqrt{1-e^{-2K_1 t}}\|d_1(t)\|_s + \frac{\delta_1}{\sqrt{2K_1}}\sqrt{1-e^{-2K_1 t}}\|y_0(t)\|_s \tag{36}$$

and

$$\begin{aligned} \|y_1(t)\| &\leq \|g_0\|\|\eta_1^{\#}\| \leq \|g_0\|\|\eta_1\| \\ &\leq \underbrace{\|g_0\|\frac{\delta_1}{\sqrt{2K_1}}\sqrt{1-e^{-2K_1 t}}\|d_1(t)\|_s}_{\gamma_1^u(\|d_1(t)\|_s)} + \underbrace{\|g_0\|\frac{\delta_1}{\sqrt{2K_1}}\sqrt{1-e^{-2K_1 t}}\|y_0(t)\|_s}_{\gamma_1^y(\|y_0(t)\|_s)} + \underbrace{\|g_0\|e^{-K_1 t}\|\eta_1(0)\|}_{\beta_1(\|\eta_1(0)\|,t)} \end{aligned} \tag{37}$$

hold. Since $\gamma_1^y \to 0$ as $K_1 \to \infty$ or $\delta_1 \to 0$, Eq. (21) holds for $\gamma_{1y} = \gamma_0^y$, $\gamma_{2y} = \gamma_1^y$ and $s_l = 0$ if proper coefficients K_1 and δ_1 are chosen. In this case, due to Theorem 1, system H_1-H_2 with (d_0, d_1) as input, (y_1, y_2) as output and (x_0, η_1) as state is IOS, and furthermore, it is easy to verify from Eqs. (33) and (36) that system H_1-H_2 is also ISS. Particularly, substituting Eq.

(34) into Eq. (37) yields[2]

$$\begin{aligned}\|y_1(t)\|_s \leq & \gamma_1^u(\|d_1(t)\|_s) + \gamma_1^y(\gamma_0^u(\|d_0(t)\|_s) + \gamma_0^y(\|y_1(t)\|_s) + \beta_0(\|x_0(0)\|, 0)) + \beta_1(\|\eta_1(0)\|, 0) \\ \leq & \gamma_1^y \circ (Id + \rho_1) \circ \gamma_0^y(\|y_1(t)\|_s) \\ & + \gamma_1^y \circ (Id + \rho_1^{-1})(\gamma_0^u(\|d_0(t)\|_s) + \beta_0(\|x_0(0)\|, 0)) + \gamma_1^u(\|d_1(t)\|_s) + \beta_1(\|\eta_1(0)\|, 0)\end{aligned} \tag{38}$$

where ρ_1 is a class $\mathcal{K}_\infty$ function. A fact to be noticed is that if Eq. (21) holds for $\gamma_{1y} = \gamma_0^y$, $\gamma_{2y} = \gamma_1^y$ and $s_l = 0$, the inequality

$$\begin{cases} \gamma_1^y \circ (Id + \rho_1) \circ \gamma_0^y(s) \leq (Id + \rho_2)^{-1}(s) \\ \gamma_0^y \circ (Id + \rho_2) \circ \gamma_1^y(s) \leq (Id + \rho_1)^{-1}(s) \end{cases}, \forall s \geq 0$$

will hold. Thus,

$$\begin{aligned}\|y_1(t)\|_s \leq & (Id + \rho_2)^{-1}(\|y_1(t)\|_s) \\ & + \gamma_1^y \circ (Id + \rho_1^{-1})(\gamma_0^u(\|d_0(t)\|_s) + \beta_0(\|x_0(0)\|, 0)) + \gamma_1^u(\|d_1(t)\|_s) + \beta_1(\|\eta_1(0)\|, 0) \\ \leq & (Id + \rho_2^{-1})(\gamma_1^y \circ (Id + \rho_1^{-1})(\gamma_0^u(\|d_0(t)\|_s) + \beta_0(\|x_0(0)\|, 0)) + \gamma_1^u(\|d_1(t)\|_s) + \beta_1(\|\eta_1(0)\|, 0))\end{aligned} \tag{39}$$

Substituting the above inequality into Eq. (33) yields

$$\begin{aligned}\|x_0(t)\| \leq & \beta_0^x(\|x_0(0)\|, t) + \alpha_0^x(\|d_0(t)\|_s) \\ & + r_m \alpha_0^x((Id + \rho_2^{-1})(\gamma_1^y \circ (Id + \rho_1^{-1})(\gamma_0^u(\|d_0(t)\|_s) + \beta_0(\|x_0(0)\|, 0)) \\ & + \gamma_1^u(\|d_1(t)\|_s) + \beta_1(\|\eta_1(0)\|, 0)))\end{aligned} \tag{40}$$

Next, the small-gain theorem will be used again to propose the final IGC law based on the former design procedures. The change of variables

$$\eta_2 = x_2 - x_2^*$$

[2]For any class $\mathcal{K}$ function γ, any class $\mathcal{K}_\infty$ function ρ such that $\rho - Id$ is of class $\mathcal{K}_\infty$, and any nonnegative real numbers a and b we have

$$\gamma(a + b) \leq \gamma(\rho(a)) + \gamma(\rho \circ (\rho - Id)^{-1}(b))$$

brings Eq. (16) into the form

$$H_3 : \begin{cases} \dot{z} = \begin{bmatrix} f_0 + g_0 x_1^{\#} \\ f_1 - \dot{x}_1^* \end{bmatrix} + \begin{bmatrix} 0_{2\times 2} & 0_{2\times 3} \\ 0_{3\times 2} & g_1 \end{bmatrix} \begin{bmatrix} 0_{2\times 1} \\ x_2^* \end{bmatrix} + \begin{bmatrix} 0_{2\times 1} \\ y_3 \end{bmatrix} + \underbrace{\begin{bmatrix} \frac{d_0}{r} \\ d_1 \end{bmatrix}}_{d_3} \\ y_2 = -\dot{x}_2^* \end{cases}$$

and

$$H_4 : \begin{cases} \dot{\eta}_2 = f_2 + g_2 u + d_2 + y_2 \\ y_3 = g_1 \eta_2 \end{cases}$$

where $z = [x_0^T, \eta_1^T]^T$. As a result of the former analysis, with x_2^*, system H_3 is ISS with respect to y_3 and d_3, and particularly, from Eq. (40), we have

$$\begin{aligned} \|x_0(t)\| \leq & \beta_0^x(\|x_0(0)\|, t) + \alpha_0^x(\|d_0(t)\|_s) \\ & + r_m \alpha_0^x((Id + \rho_2^{-1})(\gamma_1^y \circ (Id + \rho_1^{-1})(\gamma_0^u(\|d_0(t)\|_s) + \beta_0(\|x_0(0)\|, 0)) \\ & + \gamma_1^u(\|d_1(t)\|_s + \|y_3(t)\|_s) + \beta_1(\|\eta_1(0)\|, 0))) \end{aligned} \tag{41}$$

For output function y_2, the inequality

$$\|y_2(t)\| \leq \gamma_2^y(\|y_3(t)\|_s) + \gamma_2^u(\|d_3(t)\|_s) + \beta_2(\|z(0)\|, t) \tag{42}$$

holds for a pair of $\mathcal{K}$ functions (γ_2^y, γ_2^u) and a class $\mathcal{KL}$ function β_2. For system H_4, we can also design a controller based on Theorem 2 as follows

$$u = g_2^{-1}\left(-f_2 - \frac{1}{2\delta_2^2}\eta_2 - K_2\eta_2\right) \tag{43}$$

and the following inequalities hold

$$\|\eta_2(t)\| \leq e^{-K_2 t}\|\eta_2(0)\| + \frac{\delta_2}{\sqrt{2K_2}}\sqrt{1 - e^{-2K_2 t}}\|d_2(t)\|_s + \frac{\delta_2}{\sqrt{2K_2}}\sqrt{1 - e^{-2K_2 t}}\|y_2(t)\|_s \tag{44}$$

$$\begin{aligned} \|y_3(t)\| \leq & \|g_3\|\|\eta_2\| \leq \|g_3\|\|\eta_2\| \\ \leq & \underbrace{\|g_3\|\frac{\delta_2}{\sqrt{2K_2}}\sqrt{1 - e^{-2K_2 t}}\|d_2(t)\|_s}_{\gamma_3^u(\|d_2(t)\|_s)} + \underbrace{\|g_3\|\frac{\delta_2}{\sqrt{2K_2}}\sqrt{1 - e^{-2K_2 t}}\|y_2(t)\|_s}_{\gamma_3^y(\|y_2(t)\|_s)} + \underbrace{\|g_3\|e^{-K_2 t}\|\eta_2(0)\|}_{\beta_3(\|\eta_2(0)\|, t)} \end{aligned} \tag{45}$$

Due to the small-gain theorem and the form of γ_3^y, we know that if small enough δ_2 or big enough K_2 is used, Eq. (21) will hold for $\gamma_{1y} = \gamma_2^y$, $\gamma_{2y} = \gamma_3^y$ and $s_l = 0$, that is, H_3 and H_4 is IOS with respect to d_2 and d_3. Moreover, similarly to the procedure from Eq. (38) to Eq. (39), the inequality

$$\|y_3(t)\|_s \leq (Id+\rho_2^{-1})(\gamma_3^y \circ (Id+\rho_1^{-1})(\gamma_2^u(\|d_3(t)\|_s)+\beta_2(\|z(0)\|,0))+\gamma_3^u(\|d_2(t)\|_s)+\beta_3(\|\eta_2(0)\|,0)) \tag{46}$$

can be obtained. Substituting the above inequality into Eq. (41) yields

$$\begin{aligned}\|x_0(t)\| \leq & \beta_0^x(\|x_0(0)\|,t) + \alpha_0^x(\|d_0(t)\|_s) \\ & + r_m\alpha_0^x((Id+\rho_2^{-1})(\gamma_1^y \circ (Id+\rho_1^{-1})(\gamma_0^u(\|d_0(t)\|_s) + \beta_0(\|x_0(0)\|,0)) \\ & + \gamma_1^u(\|d_1(t)\|_s + (Id+\rho_2^{-1})(\gamma_3^y \circ (Id+\rho_1^{-1})(\gamma_2^u(\|d_3(t)\|_s) + \beta_2(\|z(0)\|,0)) \\ & + \gamma_3^u(\|d_2(t)\|_s) + \beta_3(\|\eta_2(0)\|,0))) + \beta_1(\|\eta_1(0)\|,0)))\end{aligned} \tag{47}$$

Since $\gamma_1^u, \gamma_1^y \to 0$ as $K_1 \to \infty$ or $\delta_1 \to 0$ and $\gamma_3^u, \gamma_3^y \to 0$ as $K_2 \to \infty$ or $\delta_2 \to 0$, it can be seen that the right-hand side of (47) approaches

$$\beta_0^x(\|x_0(0)\|,t) + \alpha_0^x(\|d_0(t)\|_s) + r_m\alpha_0^x \circ (Id+\rho_2^{-1})(\beta_1(\|\eta_1(0)\|,0)) \tag{48}$$

as $K_1, K_2 \to \infty$ or $\delta_1, \delta_2 \to 0$ for bounded d_0, d_1 and d_2, which shows that for sufficiently small δ_1, δ_2 or sufficiently big K_1, K_2 the influence of d_1 and d_2 on x_0 will be close to zero. Besides that, due to the form of α_0^x, d_0 and $\beta_1(\|\eta_1(0)\|,0)$ can be also suppressed by adjusting K_0 and δ_0.

Thus, the main results can be summarized as the following theorem.

Theorem 3 *Consider the guidance and control system (16). Assume that* $g_0(t)$ *and* $g_1(\vartheta, x_1)$

are invertible in a reasonable flight domain. For bounded $d_i(t)$ $(i = 0, 1, 2)$*, the IGC law*

$$\begin{cases} x_1^{\#*} = g_0^{-1}\left(2\dfrac{V_r}{r} - \dfrac{1}{2\delta_0^2} - K_0\right) x_0 \\ \eta_1 = x_1 - [0, (x_1^{\#*})^T]^T \\ x_2^* = g_1^{-1}\left(-f_1 - \dfrac{1}{2\delta_1^2}\eta_1 - K_1\eta_1\right) \\ \eta_2 = x_2 - x_2^* \\ u = g_2^{-1}\left(-f_2 - \dfrac{1}{2\delta_2^2}\eta_2 - K_2\eta_2\right) \end{cases} \tag{49}$$

with positive coefficients K_i *and* δ_i *for* $i = 0, 1, 2$ *can make the variables* x_0*,* η_1 *and* η_2 *be ISS with respect to* d_i $(i = 0, 1, 2)$*, and the LOS rate* x_0 *can converge into a neighborhood of zero whose size can be reduced by adjusting the coefficients* K_i *and* δ_i*.*

Remark 1 [1] introduced a set of first-order filters at each step of the traditional block backstepping approach to avoid the problem of "explosion of complexity", which made the IGC law be complex in structure. Comparing with that method, the structure of our approach is more concise.

4 Conclusions

This paper proposes a three-dimensional integrated guidance and control (IGC) approach by using small-gain theorem. The couplings between the guidance system and control system and those between different channels of the pursuer dynamics are fully and explicitly considered in the design procedure, and our IGC law can guarantee stability of the overall system including the guidance and control loop without the assumption that the angle between LOS and pursuer velocity is almost invariable. Theoretical analysis also shows that the IGC approach can make the line-of-sight (LOS) rate converge into a small neighborhood of zero, and besides, the law is more concise in structure when compared with the existing results.

References

[1] Hou, M. Z, Liang, X. L, and Duan, G. R. "Adaptive block dynamic surface control for integrated missile guidance and autopilot," *Chinese Journal of Aeronautics*, Vol. 26, No. 3, 2013, pp. 741-750.

[2] Williams, D. E., Richman, J., and Friedland, B., "Design of an integrated strapdown guidance and control system for a tactical missile," AIAA paper 1983-2169, 1983.

[3] Shtessel, Y. B., Shkolnikov, I. A., and Levant, A., "Guidance and control of missile interceptor using second-order sliding modes," *IEEE Transactions on Aerospace and Electronic Systems*, Vol. 45, No.1, 2009, pp. 110-124.

[4] Shtessel, Y. B., and Tournes, C., "Integrated higher-order sliding mode guidance and autopilot for dual-control missiles," *Journal of Guidance, Control, and Dynamics*, Vol. 45, No. 2, 2009, pp. 110-124.

[5] Shtessel, Y. B., Shkolnikov, I. A., and Levant, A., "Smooth second-order sliding modes: Missile guidance application," *Automatica*, Vol. 43, No. 8, 2007, pp. 1470-1476.

[6] Wang, X. H. and Wang, J. Z., "Partial integrated missile guidance and control with finite time convergence," *Journal of Guidance Control and Dynamics*, Vol. 36, No.5, 2013, pp. 1399-1409.

[7] Shima, T., Idan, M., and Golan, O. M., "Sliding-mode control for integrated missile autopilot guidance," *Journal of Guidance Control and Dynamics*, Vol. 29, No. 2, 2006, pp. 250-260.

[8] Idan, M., Shima, T., and Golan, O. M., "Integrated sliding mode autopilot-guidance for dual-control missiles," *Journal of Guidance Control and Dynamics*, Vol. 30, No. 4, 2007, pp. 1081-1089.

[9] Yan, H., Wang, X. H., Yu, B. F., and Ji, H. B."Adaptive integrated guidance and control based on backstepping and input-to-state stability," *Asian Journal of Control*, 2013, doi: 10.1002/asjc.682.

[10] Yan, H. and Ji, H. B. "Integrated guidance and control for dual-control missiles based on small-gain theorem," *Automatica*, Vol. 48, No. 10, 2012, pp. 2686-2692.

[11] Jiang, Z. P., Teel, A. R., and Praly, L., "Small-gain theorem for ISS systems and applications." *Mathematics of Control, Signals, and Systems*, Vol. 7, No. 2, 1994, pp. 95-120.

[12] Menon, P. K., and Ohlmeyer, E. J., "Integrated design of agile missile guidance and control systems", *Proceedings of the 7th Mediterranean Conference on Control and Automation*, Haifa, 1999, pp. 1469-1494.

[13] Palumbo, N. F., and Jackson, T. D., "Integrated missile guidance and control: A state dependent Riccati differential equation approach," *Proceedings of International Conference on Control Applications*, Hawai'i, 1999, pp. 243-248.

[14] Xin, M., Balakrishnan, S. N., and Ohlmeyer, E. J., "Integrated guidance and control of missiles with θ-D method," *IEEE Transactions on Control Systems Technology*, Vol. 14, No.6, 2006, pp. 981-992.

[15] Sontag, E. D., "Smooth stabilization implies coprime factorization," *IEEE Transactions on Automatic Control*, Vol. 34, No. 4, 1989, pp. 435-443.

[16] Li, X. G., Fang, Q., *Winged missile flight dynamics*, Xian: Northwestern Polytechnical University Press, 2004 (in Chinese).

[17] Yan, H. and Ji, H. B.,"Guidance laws based on input-to-state stability and high-gain observers," *IEEE Transactions on Aerospace and Electronic Systems*, Vol. 48, No. 3, 2012, pp. 2518-2529.